Automated Synthesis of 3′-Metalated Oligonucleotides

Elizabeth S. Krider, Jeffrey J. Rack,† Natia L. Frank,‡ and Thomas J. Meade*

Division of Biology and the Beckman Institute, California Institute of Technology, Pasadena, California 91125

Received April 13, 2001

We report the first synthesis of a metallonucleoside bound to a solid support and subsequent oligonucleotide synthesis with this precursor. Large-scale syntheses of metal-containing oligonucleotides are achieved using a solid support modified with $[Ru(bpy)_2(impy')]^{2+}$ (bpy is 2,2′-bipyridine; impy′ is 2′-iminomethylpyridyl-2′-deoxyuridine). A duplex formed with the metal-containing oligonucleotide exhibits superior thermal stability when compared to the corresponding unmetalated duplex (T_m = 50 °C vs T_m = 48 °C). Electrochemical ($E_{1/2}$ = 1.3 V vs NHE), absorption (λ_{max} = 480 nm), and emission (λ_{max} = 720 nm, τ = 44 ns, $\Phi = 0.11 \times 10^{-3}$) data for the ruthenium-modified oligonucleotides indicate that the presence of the oligonucleotide does not perturb the electronic properties of the ruthenium complex. The absence of any change in the emission properties upon duplex formation suggests that the $[Ru(bpy)_2(impy)]^{2+}$ chromophore will be a valuable probe for DNA-mediated electron-transfer studies. Despite the relatively high Ru(III/II) reduction potential, oxidative quenching of photoexcited $[Ru(bpy)_2(impy)]^{2+}$ does not lead to oxidative damage of guanine or other DNA bases.

Introduction

Recent studies of electron transfer (ET) through DNA have employed redox-active probes bound to single- and double-stranded oligonucleotides.[1−8] An important objective in this area continues to be the facile and site-specific incorporation of metal complexes into DNA. One method to achieve this goal involves the synthesis of oligonucleotides possessing metal-binding ligands, followed by incorporation of the metal complexes at these sites.[1,9−21] While this method enables the preparation of various metal-containing oligonucleotides from the same strand, it requires large amounts of metal reagent, lengthy reaction times, and multiple chromatographic separations. A second method entails the preparation of metal-containing monomers that can be incorporated during solid-phase DNA synthesis using standard phosphoramidite or H-phosphonate coupling techniques.[22−32] Advantages of this method include rapid preparation of metal-containing oligonucleotides, high yields of metal incorporation, and routine product isolation. The success of this approach depends on the synthesis of individual metalated monomers that are compatible with automated DNA synthesis techniques.

Several groups have introduced metal complexes into DNA using metalated phosphonate and phosphoramidite monomers, where the metal complex (containing Pt(II), Ru(II), or Os(II))

* To whom correspondence should be addressed.
† Present address: Department of Chemistry and Biochemistry, Ohio University, Athens, OH 45701.
‡ Present address: Department of Chemistry, Box 351700, University of Washington, Seattle, WA 98195-1700.

(1) Meade, T. J.; Kayyem, J. F. *Angew. Chem., Int. Ed. Engl.* **1995**, *34*, 352−353.
(2) Holmlin, R. E.; Dandliker, P. J.; Barton, J. K. *Angew. Chem., Int. Ed. Engl.* **1997**, *36*, 2715−2730.
(3) Fukui, K.; Tanaka, K. *Angew. Chem., Int. Ed. Engl.* **1998**, *37*, 158−161.
(4) Okahata, Y.; Kobayashi, T.; Tanaka, K.; Shimomura, M. *J. Am. Chem. Soc.* **1998**, *120*, 6165−6166.
(5) Harriman, A. *Angew. Chem., Int. Ed. Engl.* **1999**, *38*, 945−949.
(6) Kelley, S. O.; Barton, J. K. *Science* **1999**, *283*, 375−381.
(7) Tierney, M. T.; Sykora, M.; Khan, S. I.; Grinstaff, M. W. *J. Phys. Chem. B* **2000**, *104*, 7574−7576.
(8) Lewis, F. D.; Wu, T. F.; Liu, X. Y.; Letsinger, R. L.; Greenfield, S. R.; Miller, S. E.; Wasielewski, M. R. *J. Am. Chem. Soc.* **2000**, *122*, 2889−2902.
(9) Ledoan, T.; Perrouault, L.; Chassignol, M.; Thuong, N. T.; Helene, C. *Nucleic Acids Res.* **1987**, *15*, 8643−8659.
(10) Bannwarth, W.; Schmidt, D.; Stallard, R. L.; Hornung, C.; Knorr, R.; Muller, F. *Helv. Chim. Acta* **1988**, *71*, 2085−2099.
(11) Chen, C. H. B.; Sigman, D. S. *J. Am. Chem. Soc.* **1988**, *110*, 6570−6572.
(12) Telser, J.; Cruickshank, K. A.; Schanze, K. S.; Netzel, T. L. *J. Am. Chem. Soc.* **1989**, *111*, 7221−7226.
(13) Modak, A. S.; Gard, J. K.; Merriman, M. C.; Winkeler, K. A.; Bashkin, J. K.; Stern, M. K. *J. Am. Chem. Soc.* **1991**, *113*, 283−291.
(14) Jenkins, Y.; Barton, J. K. *J. Am. Chem. Soc.* **1992**, *114*, 8736−8738.
(15) Bashkin, J. K.; Frolova, E. I.; Sampath, U. S. *J. Am. Chem. Soc.* **1994**, *116*, 5981−5982.
(16) Arkin, M. R.; Stemp, E. D. A.; Pulver, S. C.; Barton, J. K. *Chem. Biol.* **1997**, *4*, 389−400.
(17) Inoue, H.; Furukawa, T.; Shimizu, R.; Tamura, T.; Matsui, M. N.; Ohtsuka, E. *Chem. Commun.* **1999**, 45−46.
(18) Wiederholt, K.; McLaughlin, L. W. *Nucleic Acids Res.* **1999**, *27*, 2487−2493.
(19) Ortmans, I.; Content, S.; Boutonnet, N.; Kirsch-De Mesmaeker, A.; Bannwarth, W.; Constant, J. F.; Defrancq, E.; Lhomme, J. *Chem. Eur. J.* **1999**, *5*, 2712−2721.
(20) Holmlin, R. E.; Dandliker, P. J.; Barton, J. K. *Bioconjugate Chem.* **1999**, *10*, 1122−1130.
(21) Khan, S. I.; Grinstaff, M. W. *J. Am. Chem. Soc.* **1999**, *121*, 4704−4705.
(22) Bannwarth, W.; Schmidt, D. *Tetrahedron Lett.* **1989**, *30*, 1513−1516.
(23) Manchanda, R.; Dunham, S. U.; Lippard, S. J. *J. Am. Chem. Soc.* **1996**, *118*, 5144−5145.
(24) Schliepe, J.; Berghoff, U.; Lippert, B.; Cech, D. *Angew. Chem., Int. Ed. Engl.* **1996**, *35*, 646−648.
(25) Magda, D.; Crofts, S.; Lin, A.; Miles, D.; Wright, M.; Sessler, J. L. *J. Am. Chem. Soc.* **1997**, *119*, 2293−2294.
(26) Meggers, E.; Kusch, D.; Giese, B. *Helv. Chim. Acta* **1997**, *80*, 640−652.
(27) Hurley, D. J.; Tor, Y. *J. Am. Chem. Soc.* **1998**, *120*, 2194−2195.
(28) Khan, S. I.; Beilstein, A. E.; Smith, G. D.; Sykora, M.; Grinstaff, M. W. *Inorg. Chem.* **1999**, *38*, 2411−2415.
(29) Khan, S. I.; Beilstein, A. E.; Sykora, M.; Smith, G. D.; Hu, X.; Grinstaff, M. W. *Inorg. Chem.* **1999**, *38*, 3922−3925.
(30) Lewis, F. D.; Helvoigt, S. A.; Letsinger, R. L. *Chem. Commun.* **1999**, 327−328.
(31) Rack, J. J.; Krider, E. S.; Meade, T. J. *J. Am. Chem. Soc.* **2000**, *122*, 6287−6288.
(32) Hu, X.; Smith, G. D.; Sykora, M.; Lee, S. J.; Grinstaff, M. W. *Inorg. Chem.* **2000**, *39*, 2500−2504.

10.1021/ic010396v CCC: $20.00
Published on Web 06/30/2001

Scheme 1[a]

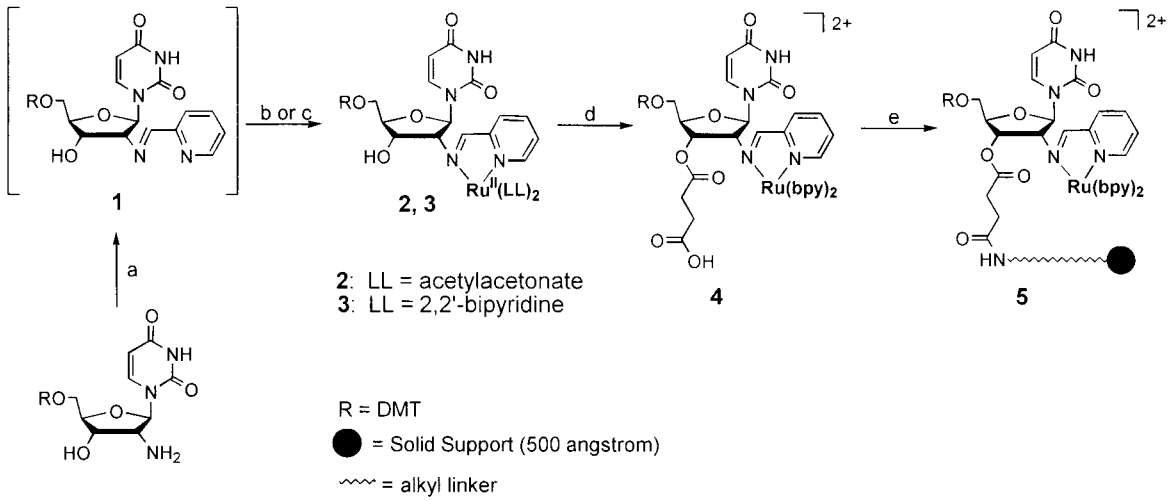

[a] Reagents: (a) 2-pyridinecarboxaldehyde, EtOH, 2 h; (b) $Ru(acac)_2(CH_3CN)_2$, EtOH, 1 h, 79% yield; (c) $Ru(bpy)_2Cl_2$, EtOH, 4 h, 19% yield; (d) succinic anhydride, DMAP, pyridine, 18 h, 54% yield; (e) solid support, TEA, HOBT, BOP, CH_2Cl_2, rt, 16 h; acetic anhydride, *N*-methylimidazole, pyridine, rt, 12 h. Metallonucleoside **2** = $Ru(acac)_2$(impy), where acac = acetylacetonate and impy = 5′-*O*-(4,4′-dimethoxytrityl)-2′-iminomethylpyridyl-2′-deoxyuridine; metallonucleoside **3** = $[Ru(bpy)_2(impy)]^{2+}$, where bpy = 2,2′-bipyridine.

is attached to the nucleoside base.[23,24,27,28,32,33] Other examples include nonnucleosidic monomers where the metal complex is tethered to the terminal phosphate group of the oligonucleotide.[22,25,26,29] Recently, we described the synthesis and spectral characterization of modified nucleosides containing low- and high-potential metal complexes (Scheme 1).[31] Importantly, these metal complexes do not lead to guanine oxidation, and are suitable electron donor/acceptor complexes. Since the site of modification is the 2′ position (as opposed to other ring positions), these metallonucleosides can be prepared as monomers for use in automated DNA synthesis.

We found that the presence of a metal complex at the 2′ ribose position decreased the coupling of phosphoramidite derivatives of these metallonucleosides.[34] Therefore, we prepared customized solid supports containing the desired metallonucleoside and used these solid supports to initiate DNA synthesis. Because oligonucleotide synthesis proceeds stepwise in a 3′ → 5′ direction beginning with the nucleoside prederivatized to the solid support, all products isolated from the DNA synthesizer contain the metal complex. This method enables the rapid production of 3′-metalated oligonucleotides, wherein the overall yield is not compromised by the coupling of a metalated phosphoramidite. Importantly, the combination of both phosphoramidite and solid-support-bound metallonucleosides will afford the automated synthesis of an oligonucleotide containing metal complexes at the 3′ *and* 5′ ends.[35]

Here we report the first synthesis of a metallonucleoside bound to a solid support and subsequent oligonucleotide synthesis with this precursor. Due to the stability of metallonucleoside **3** in the mildly acidic and strongly basic solutions that are routinely encountered during solid-phase DNA synthesis, **3** is an excellent candidate for conjugation to a solid support (Scheme 1). In contrast, the acid sensitivity of **2** precludes its use as a solid-support-bound metallonucleoside. We describe the large-scale syntheses of metal-containing oligonucleotides with a solid support modified with **3**. Interestingly, the yield is comparable to the values obtained for oligonucleotides synthesized with unmodified solid supports. A duplex formed with the metal-containing oligonucleotide exhibits greater thermal stability when compared to the corresponding unmetalated duplex. Finally, the spectroscopic properties of the single- and double-stranded metal-containing oligonucleotides are unchanged from those of the metallonucleoside complex. The automated incorporation of metallonucleoside **3** into oligonucleotides fulfills our objective of introducing a metal complex that does not oxidize the DNA bases.

Experimental Section

General Materials and Methods. All reagents were of the highest purity available from commercial sources and used as received. All solvents were of spectrophotometric quality or better. Aqueous solutions were prepared from Millipore purified water with a resistivity of 18 MΩ cm. Flash chromatography was performed on alumina (basic, activated Brockmann I, 150 mesh) from Aldrich. Thin-layer chromatography (TLC) was performed on Merck precoated silica plates (60 F_{254}, 5 × 7.5 cm). Analytical HPLC was performed using a reversed-phase Prism C18 column (Keystone Scientific, 4.6 × 250 mm, 5 μm, 100 Å), using one of the following gradients: (1) 0−17% B over 15 min, then 17−75% B over 15 min; (2) 0−100% B over 30 min; (3) 0−40% B over 15 min (A = 0.1 M triethylammonium acetate, pH 7.0, 2% acetonitrile; B = acetonitrile). Controlled pore glass (LCAA-CPG, 500 Å pore size) was obtained from Peninsula Laboratories. Oligonucleotide synthesis was carried out on an Applied Biosystems Inc. 394 DNA synthesizer using standard protocols. DNA synthesis reagents were purchased from Glen Research. Enzymes were purchased from Pharmacia.

Instrumentation. NMR spectra were recorded on a Varian 500 MHz spectrometer in the solvents noted, and chemical shifts are given relative to TMS. Steady-state absorption spectra were obtained using a Hewlett-Packard HP8452A diode array spectrophotometer. HPLC was performed using a Waters 600E controller equipped with a 994 diode array detecter. Steady-state emission spectra were obtained with a Hitatchi F-4500 fluorescence spectrophotometer using a Xe arc lamp as the light source and the following instrumental parameters: 10 nm slits, 750 V PMT, 480 nm excitation, and 500−900 nm observation range. All spectra are blank-subtracted. Quantum yield measurements were calculated using $[Ru(bpy)_3]^{2+}$ as an actinometer. Time-resolved measurements (emission and transient absorption) were conducted at the

(33) Khan, S. I.; Beilstein, A. E.; Grinstaff, M. W. *Inorg. Chem.* **1999**, *38*, 418−419.
(34) Frank, N. L.; Meade, T. J. Manuscript in preparation.
(35) Krider, E. S. Ph.D. Thesis, California Institute of Technology, Pasadena, CA, 2000.

Beckman Institute Laser Resource Center as previously described.[36] Changes in the optical density at 450 nm were monitored for the Ru(III) species generated upon oxidative quenching of the photoexcited Ru(II) species. The isosbestic point determined for **6** and **7** in the absence of quenchers was 406 nm.

Electrochemical measurements were conducted at room temperature with a CH Instruments 660 electrochemical workstation. Data were collected in a traditional two-compartment cell using a polished and sonicated 3 mm diameter glassy carbon or platinum disk working electrode (BAS), Pt wire auxiliary electrode, and Ag/AgCl reference electrode. Scan rates ranged from 0.05 to 1 V/s. Values in the text are referenced to the normal hydrogen electrode (NHE). Data for **2** were recorded in ethanol containing 0.1 M ammonium hexafluorophosphate (Aldrich); measurements of **3** were collected in either acetonitrile or dichloromethane (Burdick and Jackson) containing 0.1 M *n*-tetrabutylammonium hexafluorophosphate (SACHEM). Square-wave voltammograms of **6** or **7** were recorded in phosphate buffer (50 mM, pH 7.0, 0.5 M NaCl) in Nanopure water. Solutions were deaerated under argon.

Approximately 10−30 nmol of purified oligonucleotide was subjected to enzymatic digestion analysis. The digest cocktail (55 μL/sample) contained bacterial alkaline phosphatase (4 μL, 10 μL/unit) and snake venom phosphodiesterase (2.4 μL, 1 mL/mg), in 1 M $MgCl_2$ (0.8 μL), 0.5 M Tris buffer, pH 7.5 (3.5 μL). The reaction mixture was incubated at 37 °C for 8−16 h. The reaction was quenched by the addition of 200 μL of buffer A (see the HPLC section above), and the samples were injected after filtration. The products were analyzed by reversed-phase HPLC (gradient 1). The peaks were compared against the appropriate set of nucleoside standards for the given oligonucleotide sequence. The retention times of cytosine, thymidine, and adenosine matched those of individually injected nucleoside standards. Two peaks with identical absorption spectra were observed for the ruthenium-containing nucleoside; the sum of the integrated areas of these peaks corresponds to one ruthenium-containing nucleoside relative to the other nucleosides (ϵ_{260}(**3**) = 23300 M^{-1} cm^{-1}). The observation of two peaks is expected since the isomers of **3** and **4** were not separated prior to coupling to the solid support. Independent synthesis of the detritylated form of **3** produced two diastereomers that elute as two peaks upon HPLC injection under similar conditions (data not shown).

Thermal denaturation curves were collected using a Hewlett-Packard HP 8452A diode array spectrophotometer equipped with a Peltier temperature controller (20−70 °C range). Individual oligonucleotides were hybridized to their complementary strands in 50 mM sodium phosphate (pH 7.0) containing 0.5 M sodium chloride, to give solutions that were 2.7 μM in each strand. The samples were heated for 20 min at 70 °C and slowly cooled to 4 °C overnight. Thermal denaturation values were calculated from absorbance changes at 260 nm as the average of the heating and cooling traces collected for each hybrid; values were obtained from 2−4 separate heat−cool cycles.

Synthesis of $Ru(acac)_2$(1) (2). 5′-*O*-(4,4′-Dimethoxytrityl)-2′-amino-2′-deoxyuridine (93 mg, 0.17 mmol) was dissolved in ethanol (5 mL) containing molecular sieves, and the solution was flushed with argon for 15 min. 2-Pyridinecarboxaldehyde (15 μL, 0.16 mmol) was added incrementally, and the reaction was refluxed for 2 h. The solution was cooled, filtered to remove the molecular sieves, and evaporated to dryness under reduced pressure to give the intermediate nucleoside **1**. (Electrospray mass spectral analysis of an aliquot of crude **1** found 635.2 [M + H^+], as compared to 634.2 calculated for [M].) The nucleoside was redissolved in ethanol (5 mL), and the solution was deaerated. In a separate flask $Ru(acac)_2(CH_3CN)_2$ (0.17 mmol) was dissolved in ethanol (25 mL), and the solution was deaerated. The two solutions were combined and heated to reflux for 1 h. The solvent was removed under reduced pressure, and the green residue was purified by flash chromatography on silica using 1.5:1 THF/hexanes as mobile phase (yield 79%). ^{1}H NMR (500 MHz, $CDCl_3$): δ 8.93 (s, 1H), 8.74 (d, 1H), 7.81 (d, 1H), 7.73 (d, 1H), 7.48 (t, 1H), 7.43 (d, 2H), 7.20−7.34 (mm, 7H), 7.11 (t, 1H), 6.81 (dd, 4H), 5.36 (dd, 1H), 5.28 (s, 1H), 5.02 (s, 2H), 4.88−4.92 (m, 1H), 4.84 (s (br), 1H), 4.68−4.76 (m, 1H), 3.79 (d, 6H), 3.41−3.56 (m, 2H), 2.20 (s, 3H), 2.12 (s, 3H), 1.82 (s, 3H), 1.60 (s, 3H). UV−vis (EtOH): λ_{max} (nm) (ϵ) 234 (33400), 276 (27000), 396 (3600), 592 (3600). ESI-MS: calcd for $C_{46}H_{48}N_4O_{11}Ru$ [M + H^+] 934.96, found 934.4 [M + H^+].

Synthesis of $[Ru(bpy)_2$(1)$](PF_6)_2$ (3). 5′-*O*-(4,4′-Dimethoxytrityl)-2′-amino-2′-deoxyuridine (1.8 g, 3.31 mmol) was dissolved in ethanol (30 mL) containing molecular sieves, and the solution was flushed with argon for 15 min. 2-Pyridinecarboxaldehyde (295 μL, 3.1 mmol) was added incrementally, and the reaction was refluxed for 6 h. The solution was cooled, filtered to remove the molecular sieves, and evaporated to dryness under reduced pressure to give the intermediate nucleoside **1**. (Electrospray mass spectral analysis of an aliquot of crude **1** found 635.2 [M + $H]^+$, calcd for [M + $H]^+$ 635.14.) The residue was redissolved in EtOH (180 mL), and $Ru(bpy)_2Cl_2$ (1.6 g, 3.31 mmol) was added to the solution. The reaction was refluxed over molecular sieves for 4 h under argon. The solution was filtered, and the solvent was removed under reduced pressure. The residue was purified by flash chromatography [(a) silica, 2% saturated aqueous KNO_3, 7% water in acetonitrile; (b) basica alumina after conversion to the PF_6^- salt, 0.5% saturated aqueous KPF_6, 2.5% water in acetonitrile]. The product fractions were concentrated, dissolved in dichloromethane, and filtered to remove excess salt. The product was obtained as a red film (yield 19%). ^{1}H NMR (500 MHz, CD_3CN): δ 7.15−8.5 (mm, 31H), 6.89 (d, 4H), 6.60 (d, 1H), 6.35 (d, 1H), 5.39 (d, 1H), 4.77 (d, 1H), 4.18−4.20 (m, 2H), 3.79−3.84 (m, 6H), 2.87−3.04 (m, 2H). UV−vis (MeOH): λ_{max} (nm) (ϵ) 210 (70100), 238 (38900), 256 (25800), 284 (51900), 480 (9100). ESI-MS: calcd for $C_{56}H_{50}N_8O_7RuPF_6$ [M]$^+$ 1193.08, found 1193.0 [M]$^+$. Analytical HPLC with gradient 3: t = 24.09 min.

Synthesis of $Ru(bpy)_2$(1-succinate)$(PF_6)_2$ (4). To a solution of **3** (46.5 mg, 35 μmol) and (dimethylamino)pyridine (2.1 mg, 17.5 μmol) in 0.5 mL of anydrous pyridine was added succinic anhydride (3.1 mg, 31.5 μmol). The reaction was stirred for 19 h at room temperature under positive-pressure argon. The solvent was removed under reduced pressure, and the residue was coevaporated with toluene. The residue was purified by flash chromatography (basic alumina, 1% saturated aqueous KNO_3, 19% water in acetonitrile). The product fractions were combined, and the acetonitrile was removed. A saturated aqueous solution of ammonium hexafluorophosphate was added to the resulting solution to precipitate the product. The red solid was collected by filtration and dried under vacuum (yield 54%). ESI-MS: calcd for $C_{60}H_{54}N_8O_{10}RuPF_6$ [M]$^+$ 1293.26, found 1293.2 [M]$^+$.

Synthesis of Ru−Solid Support (5). To a solution of **4** (179 mg, 125 μmol) in 4 mL of anhydrous dichloromethane were added anhydrous triethylamine (350 μL), HOBT (22.6 mg, 166 μmol), and BOP (91, 205 μmol). This solution was transferred to a flask containing long-chain alkylamine-controlled pore glass (LCAA-CPG) (250 mg, 500 Å pore size) and agitated gently overnight at room temperature. The resin was filtered and washed with fresh dichloromethane. A portion of the rinsed CPG was removed, washed with methanol and ether, and assayed for nucleoside loading (38−47 μmol/g of resin). The remaining resin was rinsed with methanol and ether and dried under vacuum. The washed resin was resuspended in 2 mL of acetic anhydride/pyridine/THF solution (supplied by ABI) and 1 mL of 1-methylimidazole/THF solution (ABI) and was agitated for 30 min. The resin was filtered, washed with pyridine (3 × 20 mL), methanol (3 × 20 mL), dichloromethane (3 × 20 mL), and ether (3 × 20 mL), and dried under vacuum. The nucleoside loading of the solid support after capping was 28 μmol/g of resin.

Synthesis of CTCCTACACUimpyRu$(bpy)_2$ (6) and TCTCCTACACUimpyRu$(bpy)_2$ (7). Ru−solid support (40 mg, 1 μmol) was packed into an ABI column; 2−4 columns were used for each oligonucleotide synthesis. The reaction time for the first coupling was 2−10 min; the yield of the first coupling step was routinely >95%. Upon completion of the synthesis (trityl off), the contents of the columns were transferred to two glass tubes and suspended in 30% aqueous ammonia (5 mL/tube). The oligonucleotide solutions were incubated at room temperature for 15 h followed by 3 h at 55 °C. The solvent was evaporated in a speed vacuum, and the red pellets were purified by ion-exchange HPLC (Dionex NucleoPac PA-100 column; A = 10% acetonitrile in water; B = 10% acetonitrile in water, 1.5 M NH_4OAc, pH 6; 37−47% B over 17 min). The product fractions were collected,

(36) Low, D. W.; Winkler, J. R.; Gray, H. B. *J. Am. Chem. Soc.* **1996**, *118*, 117−120.

Scheme 2[a]

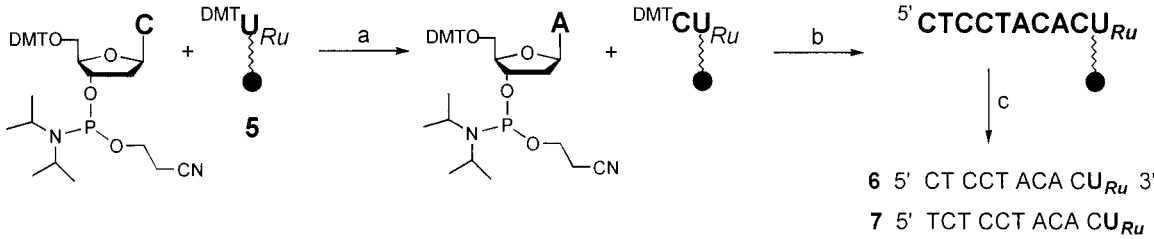

[a] Steps: (a) detritylation of **5**, monomer coupling, normal synthesis cycle; (b) detritylation of nascent oligonucleotide, monomer coupling, normal synthesis cycle; (c) cleavage of oligonucleotide from the solid support and removal of protecting groups. Oligonucleotides **6** and **7** were synthesized separately.

and the solvent was removed under vacuum. The resulting pellets were desalted using Waters C18 SepPak cartridges. Yield of **6** after isolation: 30%. MALDI−TOF MS: found 3425.73 [M − H]$^-$, calcd 3425.56 [M − H]$^-$. Yield of **7** after isolation: 28%. MALDI−TOF MS: found 3728.55 [M − H]$^-$, calcd 3730.76 [M − H]$^-$.

Results

Synthesis of the Ruthenium-Containing Solid Support. The metal-binding nucleoside **1**, 5′-*O*-(4,4′-dimethoxytrityl)-2′-iminomethylpyridyl-2′-deoxyuridine, and metallonucleoside **3** were prepared as previously described (Scheme 1).[31] A diastereomeric mixture of **3** was used in subsequent reactions and measurements. The preparation of the ruthenium-containing solid support was based on our work involving the derivatization of solid supports with 2′-substituted uridine nucleosides.[35] Treatment of **3** with succinic anhydride in the presence of DMAP[37] yielded the hemisuccinate **4** in 43% yield.[38] Derivatization of the solid support with an excess of **4** using the coupling agent BOP, followed by capping of the unreacted sites, produced the ruthenium-containing solid support **5** with high nucleoside loading (∼30 mmol/g).[39] The derivatization yield was comparable to those observed in the preparation of solid supports with similar 2′-modified nucleosides.[35]

Oligonucleotide Synthesis with 5. The preparation of 10- and 11-mer oligonucleotides containing the Ru-modified nucleoside at the 3′ terminus was performed on a 1.0 mmol scale. Automated DNA synthesis with **5** is illustrated in Scheme 2; the first coupling step lasted from 2 to 10 min. Cleavage of the products from the solid support was performed manually using concentrated aqueous ammonia. Incubation at room temperature for 15 h followed by 3 h at 55 °C provided optimal cleavage and deprotection conditions. Figure 1 shows the HPLC profile of the crude mixture of deprotected oligonucleotide **7**. The purity and composition of oligonucleotides **6** and **7** were verified by mass spectrometry and enzymatic digestion.[40] MALDI−TOF (matrix-assisted laser desorption ionization−time-of-flight) mass spectra of **6** and **7** showed a single peak representing the singly charged species and having *m*/*e* ratios equal to 3425.73 (calcd 3425.56) and 3728.55 (calcd 3730.76), respectively. HPLC analysis of the enzymatic digestion products of **6** and **7** confirmed the presence of **3** in each oligonucleotide.[40]

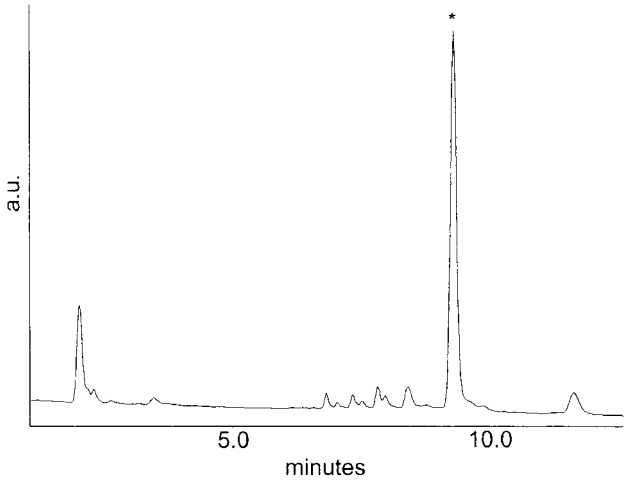

Figure 1. Ion-exchange high-pressure liquid chromatography trace of the crude mixture following synthesis, cleavage, and deprotection of oligonucleotide **7** (denoted by an asterisk; $\lambda = 260$ nm).

Absorption. The electronic spectrum of **3** displays intense UV transitions (210, 238, 256, and 284 nm) and a broad absorption band in the visible region (480 nm). The high-energy bands represent the bipyridine- and nucleoside-based $\pi-\pi^*$ transitions. The feature at 480 nm represents multiple metal-to-ligand charge-transfer (MLCT) transitions due to the presence of the bipyridine and iminomethylpyridine groups coordinated to the ruthenium center.[41−44] The electronic spectra of **6** and **7** display the same broad band in the visible region, verifying that **3** was successfully incorporated into these oligonucleotides (Figure 2). The $\pi-\pi^*$ transitions of the oligonucleotide bases are unaffected by the presence of the metal complex.

Thermal Denaturation Studies. We investigated the thermal stability of a ruthenium-containing duplex to assess the influence of the metal complex on the overall DNA structure. Table 1 shows the sequences of the duplexes prepared in 50 mM sodium phosphate buffer (pH 7.0) containing 0.5 M sodium chloride. The melting temperature (T_m) of the duplex formed by the unmodified oligonucleotide **8** and its complement **9** is 47.6 °C (Figure 3). The ruthenium-containing duplex formed by **7** and **9** exhibits a single, cooperative melting transition similar to the transition observed for the unmodified duplex. The T_m of **7·9** is 50.0 °C, 2 °C *higher* than that of **8·9**. Differences of 2−3 °C in the T_m values of metal-containing vs unmodified duplexes

(37) Abbreviations: BOP, benzotriazol-1-yloxytris(dimethylamino)phosphonium hexafluorophosphate; DBU, 1,8-diazabicyclo[5.4.0]undec-7-ene; DIEA, diisopropylethanolamine; DMAP, (dimethylamino)-pyridine; DMT, 4,4′-dimethoxytrityl; EtOAC, ethyl acetate; HOBT, hydroxybenzotriazole; TEA, triethylamine; THF, tetrahydrofuran.

(38) Caruthers, M. H.; Barone, A. D.; Beaucage, S. L.; Dodds, D. R.; Fisher, E. F.; McBride, L. J.; Matteucci, M.; Stabinsky, Z.; Tang, J.-Y. In *Methods in Enzymology: Recombinant DNA*; Grossman, R. W. a. L., Ed.; Academic Press: New York, 1987; Vol. 154.

(39) Knorr, R.; Trzeciak, A.; Bannwarth, W.; Gillessen, D. *Tetrahedron Lett.* **1989**, *30*, 1927−1930.

(40) Supporting data can be found in the Supporting Information.

(41) Brown, G. M.; Weaver, T. R.; Keene, F. R.; Meyer, T. J. *Inorg. Chem.* **1976**, *15*, 190−196.

(42) Ridd, M. J.; Keene, F. R. *J. Am. Chem. Soc.* **1981**, *103*, 5733−5740.

(43) Keene, F. R.; Ridd, M. J.; Snow, M. R. *J. Am. Chem. Soc.* **1983**, *105*, 7075−7081.

(44) The absorption features of **3** and **7** will be addressed in a forthcoming paper describing resonance Raman results.

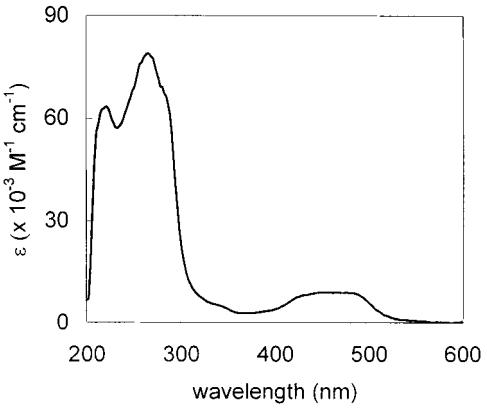

Figure 2. Absorption spectrum of oligonucleotide **7** (35 μM) at room temperature in buffer (0.05 M sodium phosphate, pH 7.0, 0.5 M sodium chloride). λ_{max} = 260 nm (ϵ = 109000 M^{-1} cm^{-1}), 480 nm (ϵ = 9100 M^{-1} cm^{-1}).

Table 1. Thermal Denaturation Temperatures for Metalated and Modified Oligonucleotides[a]

sequence	abbrev	modification	duplex	T_m (°C)[b]
5′-TCTCCTACAC**U**$_{Ru}$	**7**	3′-**U**$_{Ru}$	**7·9**	49.5 ± 0.6
5′ -TCTCCTACACT	**8**	none	**8·9**	47.6 ± 0.2
5′-AGTGTAGGAGA	**9**	none		
5′-$_a$**U**CTCCTACAC**U**$_a$	**10**	3′-**U**$_a$, 5′-**U**$_a$	**10·9**	45.8 ± 0.5
5′-$_a$**U**CTCCTACAC**U**$_b$	**11**	3′-**U**$_b$, 5′-**U**$_a$	**11·9**	46.2 ± 0.5

[a] The symbol **U**$_a$ denotes 2′-amino-2′-deoxyuridine; **U**$_b$ denotes $N^{2'}$-(2-pyridylmethyl)-2′-amino-2′-deoxyuridine. [b] Values were determined in 0.05 M sodium phosphate buffer (pH 7.0) containing 0.5 M sodium chloride; sample concentration 2.7 μM each strand.

are observed for duplexes containing other metal complexes.[12,19,27,32,33]

Electrochemistry. Voltammograms of **3** in dichloromethane display a reversible one-electron oxidation at high scan rates (1.6 V vs normal hydrogen electrode, NHE), which represents the Ru(III/II) couple. This reduction potential compares well with that reported for the model system [Ru(bpy)$_2$(impy)]$^{2+}$, where impy = iminomethylpyridine (1.5 V vs NHE, acetonitrile).[41] The Ru(III/II) reduction potential for **3** is slightly more positive than that of the model complex, suggesting that the proximity of the nucleoside to the metal center may be responsible for the small positive shift. This effect is observed for metallonucleoside **2** ($E_{1/2}$ = 0.29 V vs NHE, ethanol) and Ru(acac)$_2$(impy), where acac = acetylacetonate ($E_{1/2}$ = 0.23 V vs NHE, ethanol).[31] Incorporation of **3** into an oligonucleotide, **7**, results in a Ru(III/II) couple of 1.3 V in aqueous solution (50 mM sodium phosphate, pH 7.0, 0.5 M sodium chloride).

Multiple ligand-centered reductions are observed (−0.8, −1.1, and −1.3 V vs NHE) for **3**; the most positive reduction is irreversible. Similar results have been reported for a series of [Ru(bpy)$_2$(α,α′-diimine)]$^{2+}$ complexes.[41] On the basis of these values, estimates of the excited-state potentials of **3** are $E^{3+/2+*} \approx -0.18$ V and $E^{2+*/1+} \approx 1.0$ V vs NHE.[45]

Emission. Steady-state emission spectra of metallonucleoside **3** and oligonucleotide **7** show similar profiles. Excitation of either **3** or **7** at 480 nm produces an emission maximum at 730 nm, with a shoulder near 810 nm (Figure 4). The excited-state lifetimes are strictly monoexponential and are independent of solvent: 44 ns for **3** (aqueous methanol) and 42 ns for **7** (phosphate buffer). However, the quantum yield of **3** is slightly greater than that of **7** (Table 2). These observations support the assertion that the lowest electronically excited state is the same for both the metallonucleoside and ruthenium-containing oligonucleotide.[31]

(45) $E^*_{red} = E_{red} + E^{00}$; $E^*_{ox} = E_{ox} - E^{00}$.

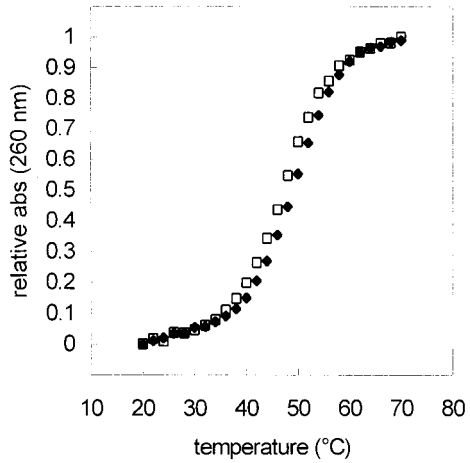

Figure 3. Thermal denaturation curves for duplex **8·9** (□) and metal-containing duplex **7·9** (◆). Sequences are given in Table 2.

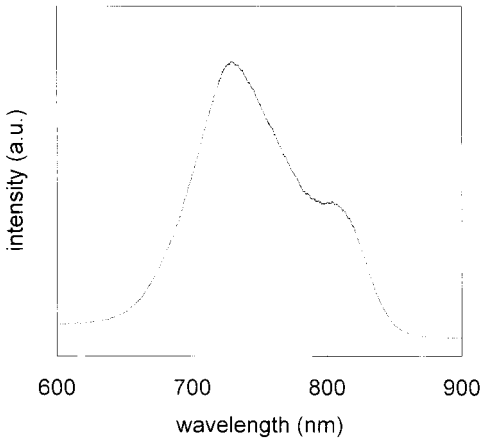

Figure 4. Steady-state emission spectrum of **3** in aerated methanol (λ_{exc} = 480 nm, λ_{max} = 730 nm).

Table 2. Absorption and Emission Data for Ru(bpy)$_2$(impy)$^{2+}$ Derivatives at Room Temperature[a]

compd	λ_{max}(abs)[b]	λ_{max}(em)[c]	τ[d]	Φ_{em}[e] × 10^{-3}
Ru(bpy)$_2$(impy)$^{2+}$	470[f]			
3	480	730	44	0.53
7	480	725	42	0.11
7·9	480	725	42	

[a] Concentrations ranged from 10 to 40 μM. [b] Measured in aqueous solution or methanol. [c] Emission maxima determined from steady-state emission spectra collected with aerated solutions (in MeOH for **3**, in water for samples containing **7**). [d] Nanoseconds (±2); lifetimes determined from monoexponential fits of the luminescence decay observed at 720 nm in degassed solutions (in 25% MeOH for **3**, in 0.05 M sodium phosphate, pH 7.0, 0.5 M NaCl for all samples containing **7**). [e] Quantum yields for emission calculated using Ru(bpy)$_3$Cl$_2$ as an actinometer. [f] Reference 41.

The absence of any significant differences in the lifetimes of **3** and **7** suggests that the bases contained in **7** (adenine, cytosine, thymine) do not quench the luminescent MLCT state. The addition of the guanine-rich complementary strand **9** to **7** does not alter the excited-state lifetime, indicating that (1) hybridization does not influence the emissive properties of the incorporated ruthenium complex and (2) the photoexcited species does not oxidize guanine, the most easily oxidized base ($E^{\bullet+/0}$ = 1.3 V vs NHE, pH 7).[46] Absorption spectra recorded at various time

points after initial excitation confirm this assessment. Moreover, data collected at multiple wavelengths do not indicate guanine oxidation.

The addition of quenchers known to generate potent Ru(III) oxidants from photoexcited ruthenium(II) polypyridyl species does not lead to detectable guanine oxidation.[47] For example, oxidative quenching of photoexcited **7·9** by $[Ru(NH_3)_6]^{3+}$ is described by linear plots of the observed decay rate constant (k_{obs}) vs quencher concentration under conditions of high ionic strength (bimolecular quenching constant $k_q = 1.1 \times 10^8$ M^{-1} s^{-1}). However, high concentrations of quencher (150−1500-fold excess of $[Ru(NH_3)_6]^{3+}$ or methyl viologen) are required to effect a ∼10% decrease in the excited-state lifetime of **7**. Absorption spectra recorded 5 μs after excitation indicate that the yield of generating Ru(III) following oxidative quenching is low.

Discussion

Incorporation Strategy. The solid-phase incorporation of nucleoside monomers containing metal complexes attached directly to the ribose ring has been unexplored until recently.[31,32] This is primarily due to the difficulty of introducing substituents to the ribose ring of the nucleoside. Nevertheless, this site is an attractive location for modifications since reporter molecules incorporated here may cause fewer perturbations to the secondary duplex structure than those attached to the nucleoside base. Additionally, the selective placement of metal complexes at various locations on the nucleoside (base and ribose positions) allows for comparative studies regarding electron-transfer pathways in nucleic acids.[48]

There are numerous constraints associated with incorporating modified nucleosides during automated solid-phase DNA synthesis.[49−52] The most demanding of these include the mildly acidic and strongly basic conditions to which the solid support is repeatedly exposed during synthesis. The choice of metallonucleoside **3** is motivated by its observed stability under these conditions. While higher yields (60−74%) for succination are observed for unmetalated nucleosides containing 2′ substituents, the modest yield for succination of **3** (43%) indicates that the metal complex inhibits this reaction (Scheme 1).[35] The successful derivatization of the solid support with the succinated metallonucleoside demonstrates that a large, cationic metal complex can be tolerated in the conjugation reaction. Succination yields for nucleosides containing metal complexes at locations other than the 2′ position are expected to be higher due to the absence of steric constraints.

The utility of solid supports prederivatized with metallonucleosides is validated by the rapid, large-scale synthesis of 10- and 11-mer oligonucleotides containing $[Ru(bpy)_2(impy')]^{2+}$ (impy′ = nucleoside **1**) complexes at the 3′ termini. Analysis of the crude oligonucleotide mixture following cleavage from the solid support reveals an efficient synthesis (integration at 260 nm indicates a yield of 70% prior to HPLC purification, as shown in Figure 1). Clearly, this methodology may be extended to other transition-metal complexes incorporated into nucleosides at either ribose or base positions, provided that the metal complex is stable to the conditions of oligonucleotide synthesis.

Effect of Metal Complexes on Duplex Stability. Thermal denaturation studies serve as an indication of how the incorporated label influences the duplex stability. In the case of duplexes containing nonintercalating metal complexes, it is difficult to ascertain from the T_m value whether the cationic nature of the metal complex partially offsets the destabilization caused by the modification. For the metal-containing duplex **7·9**, the T_m value is slightly higher than the T_m of the unmodified duplex **8·9** (50 °C vs 48 °C, respectively). Modified duplexes of similar sequence serve as a useful comparison to duplex **7·9**; they contain nucleosides with unmetalated substituents at the same ribose position (Table 1).[35] The duplexes **10·9** and **11·9** contain the modified nucleosides at both the 3′ and 5′ ends of the strands, whereas duplex **7·9** contains a single metal complex at the 3′ end. Despite the fact that the nucleosides with unmetalated 2′ substituents favor the same sugar conformation adopted by 2′-deoxynucleosides, the T_m values of the resulting duplexes are slightly below the melting temperature of the unmodified duplex.[35,53] This comparison suggests that the presence of the cationic metal complex compensates for some of the destabilizing effects induced by the 2′ modification.

Our observation that the T_m of duplex **7·9** is 2 °C higher than the T_m of the unmodified duplex **8·9** contrasts with thermal denaturation studies involving other duplexes modified with ruthenium complexes. Duplexes end-labeled with nonintercalating ruthenium complexes typically display T_m values that are essentially unchanged or lower by a few degrees compared to the values reported for unmodified duplexes.[27,32,54] For example, a 20-mer duplex containing $[Ru(bpy)_2(phen')]^{2+}$ attached to the base of the 5′-terminal nucleoside exhibits a T_m only 1 °C higher than that of the unmodified duplex (79 °C vs 78 °C).[27] The T_m values for a 16-mer duplex containing $[Ru(bpy)_2(bpy')]^{2+}$ attached to the base of the 5′-terminal nucleoside and the corresponding unmodified duplex are identical (49 °C).[54] Reductions of 2−3 °C in the T_m values are observed when similar ruthenium complexes are attached directly to the 5′ ribose position (as opposed to the base of a terminal nucleoside).[32] These results indicate that placement of nonintercalating ruthenium complexes at the 5′ ends of duplexes has only a slight destabilizing effect on duplex stability.

An exception to this trend occurs when $[Ru(bpy)_2(bpy')]^{2+}$ is tethered to the 5′-terminal phosphate group: the T_m of the metal-containing duplex is significantly lower than the value of the unmodified duplex (42 °C vs 60 °C).[29] This result suggests that tethering a cationic metal complex to the 5′-terminal phosphate group has a large destabilizing influence on the duplex. The absence of a nucleoside at the end of the duplex may be responsible for the lowered duplex stability.

Absorption. The electronic spectrum of metallonucleoside **3** displays a broad absorption band with maximum at 480 nm ($\epsilon = 9100$ M^{-1} cm^{-1}) that is red-shifted from $\lambda_{max} = 470$ nm ($\epsilon = 13600$ M^{-1} cm^{-1}) for the model complex $[Ru(bpy)_2(impy)]^{2+}$ (Table 2).[42] The slight difference in λ_{max} for the model complex and the metallonucleoside reveals the effect of replacing the impy ligand with an impy derivative possessing a ribose substituent on the imino nitrogen. The metal-containing oligonucleotides **6** and **7** display visible absorption bands identical

(46) Steenken, S.; Jovanovic, S. V. *J. Am. Chem. Soc.* **1997**, *119*, 617−618.
(47) Bock, C. R.; Meyer, T. J.; Whitten, D. G. *J. Am. Chem. Soc.* **1974**, *96*, 4710−4712.
(48) Krider, E. S.; Meade, T. J. *J. Biol. Inorg. Chem.* **1998**, *3*, 222−225.
(49) *Oligonucleotide Synthesis: A Practical Approach*; Gait, M., Ed.; Oxford University Press: Oxford, 1984.
(50) Goodchild, J. *Bioconjugate Chem.* **1990**, *1*, 165−191.
(51) *Oligonucleotides and Analogues: A Practical Approach*; Eckstein, F., Ed.; Oxford University Press: Oxford, 1991.
(52) Detailed descriptions of oligonucleotide synthesis are given in refs 49−51.
(53) Saenger, W. *Principles of Nucleic Acid Structure*; Springer-Verlag: New York, 1984.
(54) Khan, S. I.; Beilstein, A. E.; Tierney, M. T.; Sykora, M.; Grinstaff, M. W. *Inorg. Chem.* **1999**, *38*, 5999−6002.

Table 3. Absorption and Emission Data for Ruthenium(II) Polypyridyl Complexes Incorporated into Oligonucleotides[a]

compd	λ_{max}(abs)	λ_{max}(em)	τ (μs)	ref
$Ru(bpy)_3^{2+}$	452	628	0.65	55
$Ru(bpy)_2(impy)^{2+}$	470			41
3[b]	480	730	0.044	
7	480	725	0.042	
7·9	480	725	0.042	
$Ru(bpy)_2(bpy')^{2+}$	460	670	0.407	29
5′-^{X}TCAACAGTTTGTAGCA	465	670	0.616	29
duplex			0.629	29
$Ru(bpy)_2(bpy')^{2+}$	454	675	0.485	29,54
5′-TCAACAG^{X}TTGTAGCA	450	660	0.544	29,54
duplex			0.594	29,54
$Ru(bpy)_2(bpy')^{2+}$	450	666	0.430	58
5′-^{X}TCAACAGTTTGT	450	677	0.572	58
duplex			0.586	58
$Ru(bpy)_2(bpy')^{2+}$[c]	468	665	0.850	30
5′-TTTT-**X**-AAAA	468	665	0.815	30
5′-GGG-**X**-CCC	468	665	0.790	30
5′-GCAATTGC-**X**-GCAATTGC	468	665	0.608	30
$Ru(bpy)_2(phen')^{2+}$[d]	450	629		27
5′-TCGGCGCGAA^{X}TCGCGTGCC	456	630		27
duplex				27
$Ru(bpy)_2(bpy')^{2+}$	460	660		12
5′-GCAC^{X}TCAG	460	660		12
duplex				12

[a] Values measured in buffered aqueous solution (pH 7.0) at room temperature unless otherwise noted. **X** denotes metal attachment to the oligonucleotide via a linker to the nucleoside base, ribose, or phosphate. Please see individual references for details of metal attachment for each system. [b] Measured in aqueous methanol solution. [c] Measured in unbuffered aqueous solution. [d] Monomer complex values measured in acetonitrile.

to those of **3**, demonstrating that incorporation does not alter the electronic properties of the metallonucleoside.

Similar trends are observed for oligonucleotides containing derivatives of $[Ru(bpy)_3]^{2+}$. Changes in the absorption maximum occur when the model complex (i.e., $[Ru(bpy)_3]^{2+}$) is modified to accommodate linkers required for oligonucleotide attachment (Table 3). The resulting monomer complex (i.e., $[Ru(bpy)_2(bpy')]^{2+}$, where bpy′ denotes a substituted bipyridine ligand containing the linker) displays an absorption maximum that is unchanged or slightly red-shifted from λ_{max} for $[Ru(bpy)_3^{2+}]$.[55] Typically, incorporation of the monomer complex into an oligonucleotide does not alter λ_{max} for the metal-containing oligonucleotides (Table 3).

Emission. The emission spectra of **7** and **7·9** are virtually identical to that of the precursor **3**, indicating that both incorporation into an oligonucleotide and hybridization of the metal-containing strand do not alter the emissive properties of the metal complex (Table 1). This result is in contrast to the changes in the emissive behavior of monomer complexes based on $[Ru(bpy)_3]^{2+}$ (Table 3). In most cases, these complexes exhibit emission maxima shifted from 628 nm to lower energy (660−675 nm). When the monomer complexes are incorporated into oligonucleotides, the emission maxima are unchanged or shifted to lower energy. An exception to this trend is a 16-mer oligonucleotide containing a $[Ru(bpy)_2(bpy')]^{2+}$ complex attached to the base of a nucleoside located midstrand; the emission maximum is centered at 660 nm, blue-shifted from the corresponding value of the monomer complex (675 nm).[28,54]

The excited-state lifetime of **3** does not change upon incorporation into an oligonucleotide and subsequent duplex formation. This result contrasts with observations made for many of the metal-containing oligonucleotides in Table 3. The lifetimes of both single- and double-stranded oligonucleotides are dramatically different from those of the monomer complexes, despite identical experimental conditions. For example, Grinstaff and co-workers report an increase in the lifetime values upon both incorporation and hybridization of three separate $[Ru(bpy)_2(bpy')]^{2+}$ derivatives, regardless of the attachment linkage or placement of the metal complex within the duplex.[29,32,54] Conversely, Lewis and co-workers observe a decrease in the lifetime of single-stranded oligonucleotides containing a $[Ru(bpy)_2(bpy')]^{2+}$ label.[30] The lifetimes of two short strands are within 10% of the value for the monomer complex; a third strand forms a hairpin structure at high ionic strength and exhibits a lifetime that is 30% shorter compared to the lifetime of the monomer complex.

A rationale for the contrasting changes in the excited-state lifetime values of the metal-containing oligonucleotides summarized in Table 3 is unclear. The decrease in excited-state lifetime reported by Lewis for the single-stranded vs hairpin oligonucleotides could be attributed to structural differences between the conformations available to the strands. The two 8-mer strands do not form well-defined hairpin structures at high ionic strength; therefore, the emission lifetimes for these oligonucleotides are expected to resemble that of the monomer complex.[30] The 16-mer oligonucleotide forms a stable hairpin structure, and this structural difference may cause the observed decrease in the excited-state lifetime.[56] However, the increase in lifetime values upon both incorporation and hybridization reported by Grinstaff may be due to interactions between the metal complex and the duplex not operative in Lewis' hairpin assembly. Subtle factors involving duplex conformation and ionic strength may be responsible for these trends.

Guanine Oxidation. The absence of any significant differences in the lifetimes of **3**, **7**, and **7·9** suggests that the bases contained in **7** or **9** do not quench the photoexcited $[Ru(bpy)_2(impy')]^{2+}$. Although guanine is the most facile electron donor of the DNA bases ($E^{\bullet+/0} = 1.3$ V vs NHE, pH 7),[46] oxidation by photoexcited **7** is not favored thermodynamically ($E^{2+*/1+} \approx 1.0$ V vs NHE). Even the addition of oxidative quenchers to this assembly fails to result in any oxidative damage to the DNA bases of **7·9**, despite generating a Ru(III) species that is a powerful oxidant ($E_{1/2} = 1.3$ V vs NHE, buffered aqueous solution).

Modest decreases in the excited-state lifetimes of **7** and **7·9** are observed in the presence of a large excess of oxidative quenchers. In the case of $[Ru(NH_3)_6]^{3+}$, the bimolecular quenching constant determined for the quenching of photoexcited **7·9** is 1 order of magnitude smaller compared to the value measured for the quenching of $[Ru(bpy)_3]^{2+}$ (1.1×10^8 M^{-1} s^{-1} vs 2×10^9 M^{-1} s^{-1}, respectively).[47] However, the driving force estimate (ΔG_q) for the single electron transfer from $[Ru(NH_3)_6]^{3+}$ to photoexcited **7·9** is approximately −0.24 eV, much smaller than the value calculated for $[Ru(bpy)_3]^{2+*}$ (−0.92 eV).[47,57] Oxidative quenching by methyl viologen is thermodynamically unfavorable ($\Delta G_q = 0.26$ eV). Despite the large difference in ΔG_q for the two quenchers, the addition of either quencher in large excess to **7** or **7·9** generates small amounts of oxidized product.

(55) Juris, A.; Balzani, V.; Barigelletti, F.; Campagna, S.; Belser, P.; Vonzelewsky, A. *Coord. Chem. Rev.* **1988**, *84*, 85−277.

(56) An estimate of the excited-state reduction potential of $[Ru(bpy)_2(bpy')]^{2+}$, based on data collected for $[Ru(bpy)_3]^{2+}$, suggests that guanine oxidation from the excited state is not likely (ref 55).

(57) $\Delta G_q = -[E_{1/2}^{Q/Q^-} - E_{1/2}^{Ru^{3+}/Ru^{2+*}}]$.

(58) Hu, X.; Smith, G. D.; Sykora, M.; Lee, S. J.; Grinstaff, M. W. *Inorg. Chem.* **2000**, *39*, 2500−2504.

Conclusion

The goal of this work is to develop a facile method for incorporating redox-active probes into oligonucleotides that do not oxidize DNA. We report the first method of synthesizing a metal-containing solid support for use in automated DNA synthesis. This achievement represents a significant advance in the development of metal-containing oligonucleotides. While the solid support employed here is glass-based, the method is applicable to other solid supports containing long-chain alkylamine linkers. This methodology can be extended to other transition-metal complexes incorporated into nucleosides at either ribose or base positions, provided that the metal complex is stable to the conditions of oligonucleotide synthesis. The preparation of a metal-containing solid support provides the opportunity to generate oligonucleotides with metal complexes placed at the 3′, intervening, and 5′ positions of the duplex when combined with other solid-phase incorporation methods.

Thermal denaturation studies of the modified duplexes indicate that the presence of metallonucleoside **3** at the 3′ terminus compensates for part of the destabilizing effects induced by placing a chelating ligand at the 2′ ribose position. The metal-containing strands exhibit electrochemical and spectroscopic features nearly identical to those of the individual metallonucleoside. The absence of any change in these properties upon metallonucleoside incorporation into oligonucleotides and subsequent hybridization suggests that the $Ru(bpy)_2(impy)^{2+}$ chromophore is a valuable probe for DNA-mediated ET studies.

Acknowledgment. We thank Harry B. Gray and Jay R. Winkler for helpful discussions. E.S.K. thanks Timothy Hubin and Pratip Bhattacharya for technical assistance. This work was supported by NIST (ATP) Award 70NANB5H1031, the Jet Propulsion Laboratory (JPL 67192), and the Beckman Institute Biological Imaging Center.

Supporting Information Available: Instrumental details and experimental data for complexes **2**−**7**. This material is available free of charge via the Internet at http://pubs.acs.org.

IC010396V